



**HAL**  
open science

# From calorimetry to thermal risk assessment: $\gamma$ -Valerolactone production from the hydrogenation of alkyl levulinates

Yanjun Wang, Igor Plazl, Lamiae Vernières-Hassimi, Sébastien Leveneur

## ► To cite this version:

Yanjun Wang, Igor Plazl, Lamiae Vernières-Hassimi, Sébastien Leveneur. From calorimetry to thermal risk assessment:  $\gamma$ -Valerolactone production from the hydrogenation of alkyl levulinates. *Process Safety and Environmental Protection*, 2020, 144, pp.32-41. 10.1016/j.psep.2020.07.017 . hal-03144825

**HAL Id: hal-03144825**

**<https://normandie-univ.hal.science/hal-03144825>**

Submitted on 6 Jan 2022

**HAL** is a multi-disciplinary open access archive for the deposit and dissemination of scientific research documents, whether they are published or not. The documents may come from teaching and research institutions in France or abroad, or from public or private research centers.

L'archive ouverte pluridisciplinaire **HAL**, est destinée au dépôt et à la diffusion de documents scientifiques de niveau recherche, publiés ou non, émanant des établissements d'enseignement et de recherche français ou étrangers, des laboratoires publics ou privés.

1 **From calorimetry to thermal risk assessment:  $\gamma$ -valerolactone production**  
2 **from the hydrogenation of alkyl levulinate**

3

4 *Yanjun Wang<sup>1</sup>, Igor Plazl<sup>2</sup>, Lamiae Vernières-Hassimi<sup>1</sup>, Sébastien Leveneur<sup>1\*</sup>*

5 *<sup>1</sup>Normandie Univ, INSA Rouen, UNIROUEN, LSPC, EA4704, 76000 Rouen, France, E-mail :*

6 [sebastien.leveneur@insa-rouen.fr](mailto:sebastien.leveneur@insa-rouen.fr)

7 *<sup>2</sup>Faculty of Chemistry and Chemical Technology, University of Ljubljana, Večna pot 113, 1000*

8 *Ljubljana, Slovenia*

9

10 **Abstract.**

11 The use of lignocellulosic biomass as a raw material can sustain the chemical industry. There is a  
12 lack of knowledge in kinetics and thermodynamics of some of these processes, making difficult  
13 the cost analysis. For instance, the thermodynamic investigation of the hydrogenation of alkyl  
14 levulinates to  $\gamma$ -valerolactone (GVL) is seldom. This system is a two-step reaction comprising a  
15 hydrogenation and cyclization step. The experimental measurement of the two reaction enthalpies  
16 is challenging, and a method was developed in this manuscript. The hydrogenation of methyl  
17 levulinate (ML) and butyl levulinate (BL) in the GVL solvent was found to be an exothermic step,  
18 and the cyclization an endothermic one. The reaction enthalpy for the hydrogenation of ML in the  
19 GVL solvent, calculated to -53.25 kJ/mol, is higher than the one of BL in the GVL solvent,  
20 calculated to -38.66 kJ/mol. The reaction enthalpies for the cyclization step are similar for ML  
21 and BL system, i.e., +7.00 kJ/mol and +6.50 kJ/mol, respectively. Hence, the hydrogenation step  
22 governs the reaction temperature. A thermal risk assessment based on experiments performed  
23 under adiabatic condition was done. The thermal risk was found to be medium for this reaction  
24 system under the operating conditions used in this study.

25

26 **Keywords:** reaction enthalpies, calorimetry, biomass valorization, thermal risk, kinetic  
27 modeling,  $\gamma$ -valerolactone production

28

29 **Highlights**

30

31 - Determination of the reaction enthalpy of the first and second steps for the hydrogenation  
32 of methyl and n-butyl levulinate.

33 - Development of kinetic models for the hydrogenation of methyl and n-butyl levulinate  
34 over Ru/C catalyst under adiabatic conditions.

35 - The thermal risk was evaluated to be medium for the hydrogenation of methyl and n-butyl  
36 levulinate.

37

38 **1. INTRODUCTION**

39

40 The use of biomass as a raw material for the production of chemicals, fuels and materials can be  
41 seen as a game-changer in the chemical industry. From an environmental viewpoint, these raw  
42 materials are more ecofriendly than fossil raw materials because they are renewable. From a  
43 societal and political viewpoint, the use of local biomass could revitalize rural areas and create  
44 new jobs (Budzianowski and Postawa, 2016).

45 The choice of biomass raw material is crucial and must respect several criteria, such as:

46 - The cultivation of this biomass should not lead to soil and groundwater pollution.

47 - The biomass should not be used in the alimentary sector.

48 - An optimum synergy between the harvest, transportation and storage should be found.

49 - A total valorization of the biomass must be done.

50 In order to avoid the dilemma of food versus fuel, the use of second-generation biomass as a raw  
51 material in the chemical industry should be privileged. Second-generation biomass can be  
52 lignocellulosic biomass, agricultural waste, or dedicated non-food crops (miscanthus, switchgrass)  
53 on non-agricultural lands.

54 The valorization of lignocellulosic biomass at the industrial scale has considerably increased these  
55 recent years (Chandel et al., 2020). One of the main challenges is the pretreatment step to separate  
56 lignin, cellulose, and hemicellulose for further upgrading into valuable chemicals, fuels, or  
57 materials. One can mention the commercial-scale cellulosic ethanol production plant by GranBio  
58 company in Brazil, with a capacity production of 82 million liters per year (GranBio, 2014).  
59 Energy cane, straw and sugarcane bagasse can be used as raw materials. These raw materials were

60 pretreated by steam explosion, and then enzymatic processes were used for hydrolysis and  
61 fermentation steps. Another successful lignocellulosic industrial application is the Borregaad  
62 plant in Sarpsborg (Norway), producing vanillin via the sulfite pulping method (Wong, 2012).  
63 This plant has a production capacity of 250 tonnes per year and used spruce trees as feedstocks  
64 (Borregaard, 2019).

65 Another promising molecule produced from lignocellulosic biomass and more specifically from  
66 cellulose and hemicellulose is levulinic acid, which was classified as a top 10 building blocks or  
67 platform molecules by the U.S. Department of Energy (Gallezot, 2012). Levulinic acid is  
68 industrially produced from the acid hydrolysis of cellulose (Hayes et al., 2005). At the industrial  
69 scale, GFBiochemicals is the main company to produce this molecule (ca. 10000 tonnes per year)  
70 via ATLAS Technology™ (Makhubela and Darkwa, 2018; Pulidindi and Kim, 2020). There is  
71 also a growing interest to study the production of alkyl levulinates from the alcoholysis of  
72 cellulose or hemicellulose (Peng et al., 2011; Wu et al., 2012; Ding et al., 2015; An et al., 2017;  
73 Di Bitonto et al., 2018). These levulinates are still considered as platform molecules with the  
74 primary benefits to be less corrosive than levulinic acid.

75 Further upgrading of levulinic acid or alkyl levulinates is by hydrogenation to  $\gamma$ -valerolactone  
76 (GVL). This molecule is of particular interest because it is also a platform molecule (Yan et al.,  
77 2015). Indeed, GVL can be used as fuel additives and solvents and has excellent potential for  
78 further upgrading to valuable chemicals, materials, and fuels (Bozell et al., 2000; Huber et al.,  
79 2006; Horváth et al., 2008; Bond et al., 2010; Serrano-Ruiz et al., 2010; Alonso et al., 2012; Qi  
80 and Horváth, 2012; Wettstein et al., 2012; Luterbacher et al., 2014; Mellmer et al., 2014; Tukacs  
81 et al., 2015; Rodenas et al., 2018; Sener et al., 2018; Al-Naji et al., 2019)

82

83



107 In a previous study, it was shown that hydrogenation of levulinic acid in water solvent could  
108 present a severe risk of thermal runaway according to the operating conditions (Wang et al., 2018)  
109 The assessment of such risk must be done. Indeed, Dakkoune et al. demonstrated that this risk is  
110 responsible for around 25% of the accident in the French chemical plants (Dakkoune et al., 2018)  
111  
112 For quantifying a thermal risk, one needs to calculate/estimate probability and severity parameters  
113 under adiabatic conditions and in batch mode, i.e., the worst-case scenario (Stoessel, 2008;  
114 Leveneur et al., 2016). The knowledge of the Time-to-Maximum Rate under adiabatic conditions  
115 ( $TMR_{ad}$ ) parameter can assess the probability of thermal runaway (Stoessel, 2008). This  
116 parameter is defined as the time to reach the maximum temperature rate. The adiabatic  
117 temperature rise under adiabatic condition ( $\Delta T_{ad}$ ) is a parameter evaluating the severity of the  
118 thermal risk. To estimate these thermal risk parameters at different operating conditions, one  
119 needs to investigate kinetics (reaction order, rate constants, activation energy...) and  
120 thermodynamics (specific heat capacity, reaction enthalpy...) of a chemical system.  
121 There are several strategies to obtain these parameters. The most widespread approach is to  
122 perform some experiments in an adiabatic calorimeter and apply a zero-order approach to estimate  
123  $TMR_{ad}$  and  $\Delta T_{ad}$ . The main drawback of such an approach is that one cannot estimate the values  
124 of these parameters at different operating conditions (Vernières-Hassimi et al., 2017).  
125  
126 The other issue concerning the determination of these parameters comes from the experimental  
127 part. Kinetic models can be developed based on experiments performed under isothermal  
128 conditions at process temperatures, and thermodynamic constants could be measured in  
129 calorimeter or evaluated via thermodynamic models. However, this approach is not representative  
130 of a thermal runaway because one can miss the observation of secondary reactions or other side  
131 reactions occurring at higher temperatures, which could worsen the accident (Stoessel, 2008).

132 The thermal runaway assessment must be done based on experiments performed under adiabatic  
133 conditions. For that, there are several calorimeters: ARSST (Marco et al., 2000; Tang et al., 2009;  
134 Veedhi and Sawant, 2013; Veedhi et al., 2014; Vernières-Hassimi et al., 2017; Leveneur, 2017;  
135 Leveneur et al., 2018; Wang et al., 2018; Shen et al., 2019; Pérez-Sena et al., 2020), VPS2  
136 (Delhaye et al., 2007; Wu et al., 2008; Chi et al., 2009; Jhu et al., 2012; Tseng et al., 2012; Liu et  
137 al., 2013; Zhang et al., 2017), PhiTecII (Singh, 1993; Sempere et al., 1997; Maestri et al., 2006;  
138 ReyesValdes et al., 2016; Saha et al., 2018; Sun et al., 2019) and RC1 (Lunghi et al., 2002; Wang  
139 et al., 2019; Wang et al., 2020). The main challenge for the gas-liquid-solid system is the mixing  
140 issue. High-pressurized RC1 Mettler-Toledo can ensure an efficient mixing for the hydrogenation  
141 of levulinic acid or alkyl levulinates over Ru/C.

142

143 In this manuscript, thermal risk assessments of methyl levulinate and butyl levulinate  
144 hydrogenation to GVL over Ru/C were conducted. These two alkyl levulinates can be produced  
145 from the alcoholysis of cellulose and are less corrosive than GVL. The benefit of the GVL solvent  
146 is its low vapor pressure value with temperature, high flash point (96°C), and low melting point  
147 (-31°C). GVL is considered a promising solvent (Horváth et al., 2008; Lin et al., 2017; Pokorný  
148 et al., 2017; Chew et al., 2020; Liu et al., 2020). In a previous study of our group (Wang et al.,  
149 2019), it was demonstrated that hydrogenation of these alkyl levulinates in GVL over Ru/C is a  
150 two-step reaction, as illustrated by Scheme 1. Some experiments were performed in RC1 Mettler-  
151 Toledo under isothermal and adiabatic conditions. To the best of our knowledge, the use of  
152 adiabatic conditions with such reaction volume is rare in the literature.

153

154 In the first stage, a methodology was developed to experimentally measure the reaction enthalpy  
155 of each reaction step for ML and BL hydrogenation system in GVL. Two different calorimeters  
156 were used for this stage: RC1 calorimeter and Tian-Calvet calorimeter.

157 In the second stage, kinetic models for both substrates were developed based on experiments in  
158 RC1 under adiabatic conditions. From the estimated kinetic constants and measured  
159 thermodynamic constants, thermal risk assessment was performed.

160

161

162

163        **2. EXPERIMENTAL SECTION**

164        **2.1 Chemicals**

165

166 Methyl levulinate (wt%  $\geq$  98%) and  $\gamma$ -valerolactone (wt%  $\geq$  99%) were purchased from  
167 Sigma-Aldrich. Alfa Aesar provided n-Butyl levulinate (wt%  $\geq$  98%). Acros Organics supplied  
168 furfural (wt%  $\geq$  99%). Alfa Aesar provided Ru/C (5 wt % ruthenium on activated carbon powder,  
169 reduced and 50% water wet). Linde supplied H<sub>2</sub> (>99.999%). Acetone (Analytical grade) was  
170 bought from VWR. Sulfuric acid (wt%  $\geq$  98%) was obtained from Fisher chemicals. All the  
171 chemicals were used without further treatment.

172

173        **2.2 RC1 experiments**

174

175 Hydrogenation of ML or BL to GVL catalyzed over Ru/C in the GVL solvent was performed in  
176 RC1, which includes pressure system, temperature system and process control system (Fig. 1).  
177 The experiments were performed under isothermal or adiabatic, and isobaric conditions assured  
178 by the process control system and jacket temperature control system. A gas entrainment impeller  
179 was used to ensure efficient gas-liquid mixing.

180

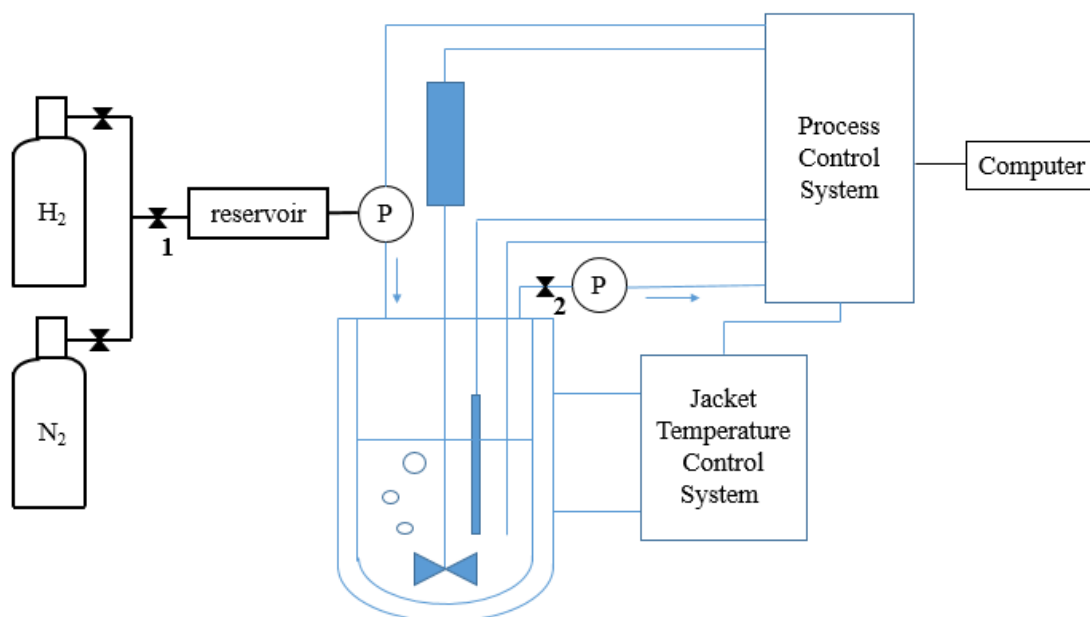


Fig. 1 - RC1 for hydrogenation of ML or BL to GVL.

181

182

183

### 184 2.2.1 Experiments under isothermal conditions

185

186 At first, an alkyl levulinate solution was introduced to the reactor with the Ru/C catalyst. Then,  
 187 the sealed reactor was purged with nitrogen three times before increasing temperature in the  
 188 reactor to 130°C. The stirring was stopped, and valve 2 was closed when the reactor temperature  
 189 reached 130°C. After that, valve 1 was open, and ca. 35 bar of hydrogen was injected into the  
 190 reactor. When reaching 35 bar in the reactor, valve 1 was closed, and the pressure in the reservoir  
 191 was around 70 bar. In this way, the storage gas in the reservoir was enough to maintain the  
 192 pressure constant in the reactor during the reaction by the automatic pressure control system. The  
 193 stirring was fixed to 800 rpm to start the reaction. Under isothermal condition, the jacket  
 194 temperature control system was set to keep the reaction temperature constant. During the reaction  
 195 time, no sample was taken to avoid any interferences with the reaction temperature signal.

196

197

198 GC analyzed the initial and final reaction mixture. Table 1 shows the operating conditions for  
 199 both experiments in the RC1 calorimeter.

200

201 Table 1. Operating conditions for the hydrogenation of alkyl levulinate under isothermal and  
 202 isobaric conditions in RC1.

Levulinates	Initial concentration (mol/L)			Catalyst loading in dry basis (kg/L)	Temperature (°C)	Pressure (Bar)
	Substrate	GVL	Alcohol			
ML	5.15	3.90	0	$5.28 \times 10^{-3}$	130	35
BL	2.04	6.79	0	$5.43 \times 10^{-3}$	130	35

203

### 204 2.2.2 Experiments under adiabatic condition

205

206 The alkyl levulinate solution was introduced into the reactor, followed by a nitrogen purge. The  
 207 initial reaction temperature was set to 100 °C under adiabatic mode. Experiments were carried out  
 208 under isobaric conditions at 35 bar. The stirring speed was set at 800 rpm to start the reaction. No  
 209 samples were withdrawn during adiabatic experiments. Table 2 shows the operating conditions  
 210 for both experiments in the RC1 calorimeter under adiabatic conditions.

211 Table 2. Operating conditions for the hydrogenation of alkyl levulinates under adiabatic and  
 212 isobaric conditions in RC1.

	Initial concentration (mol/L)			Catalyst loading in dry basis (kg/L)	Initial temperature (°C)	Pressure (Bar)
	Substrate	GVL	Alcohol			
ML	4.64	3.69	0	$5.42 \times 10^{-3}$	100	35
BL	4.28	1.81	0	$5.43 \times 10^{-3}$	100	35

213

214 **2.3 C80 experiments**

215

216 Cyclization experiments were performed in the Tian-Calvet calorimeter C80 (Fig. 2) (Zheng et  
217 al., 2016). The calorimeter C80 is a differential calorimeter operating under isothermal condition  
218 and requires a small amount of reaction mixture (1g). To only measure the heat flow rate due to  
219 reaction 2, solutions with a high concentration of intermediates were prepared. For that, the RC1  
220 calorimeter was used, and the reaction was stopped before the full conversion of the intermediate  
221 to GVL. Then, the solution was filtered to remove the heterogeneous catalyst. The solutions were  
222 stored in a fridge to quench the cyclization reaction. Table 3 shows the operating conditions for  
223 experiments in the C80.

224

225 Hastelloy cells were used: one reference cell and one measurement cell. The temperature and heat  
226 flow rate was monitored during the experiments. For this study, the experiments were performed  
227 at 60°C to avoid liquid evaporation and cyclization reaction in the reference cell.

228 Table 3. Operating conditions for the ring closure experiments in C80 under isothermal  
229 conditions for the inside tube.

	Initial concentration (mol/L)			Temperature (°C)
	Substrate	GVL	Intermediate	
<b>ML</b>	0	7.80	1.70	60
<b>BL</b>	0.17	9.01	0.33	60

230

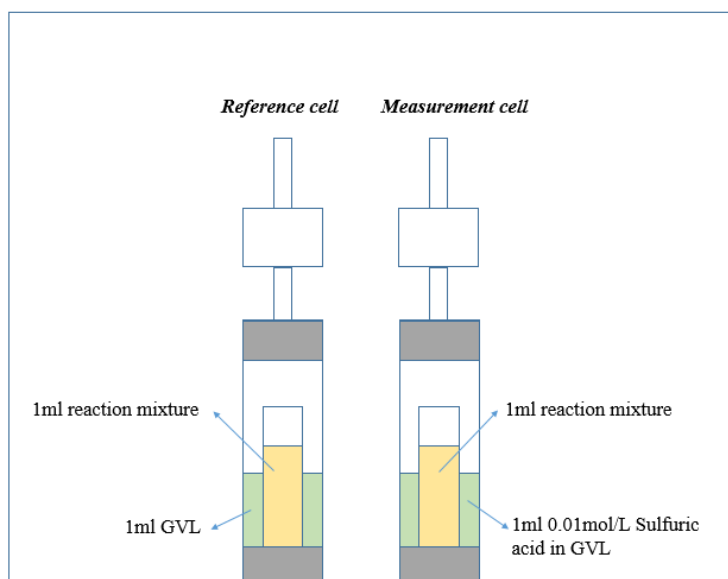


Fig. 2 - Cyclization reaction performed in C80.

231

232

233 The cell contains two major parts: inside an open tube and an outside container (Fig. 2). For the  
 234 measurement cell, the inside tube was filled with 1 mL of the reaction mixture, and the outside  
 235 was filled with 1 mL of sulfuric acid solution in GVL concentrated at 0.01 mol.L<sup>-1</sup>. Sulfuric acid  
 236 was used to catalyze the cyclization to obtain a neat signal. For the reference cell, the inside tube  
 237 was filled with 1ml of the reaction mixture, and the outside container was filled with 1ml of pure  
 238 GVL. The reference cell must have a similar specific heat capacity ( $m \times C_p$ ) than the measurement  
 239 one, and no reaction must occur in this cell. At this temperature and in the absence of catalyst, the  
 240 cyclization kinetics is negligible. This absence of reaction in the reference cell was confirmed by  
 241 GC analysis.

242 After the preparation of the cells, they were put inside the C80 calorimeter vertically, and the  
 243 temperature of this calorimeter was fixed to 60°C. When the temperature reached 60°C, and the  
 244 heat flow rate was stable, the calorimeter started to rotate continuously. When this rotating process  
 245 started, the liquids in the inside tube and outside container were mixed, and the reaction started.  
 246 After ca. 3h reaction, the rotating was stopped, and the calorimeter was cooled down. A GC  
 247 analysis was carried out on the initial and final reaction mixture from the reference and  
 248 measurement cells.

249        **2.4 Analytical section**

250

251    The concentration of substrates (ML, BL), intermediates (MHP, BHP), and GVL was quantified  
252    by GC-FID analysis. Samples were filtered and diluted with acetone. Furfural was used as an  
253    internal standard for quantification. Bruker Scion GC436 gas chromatography (GC) equipped  
254    with an FID detector (flame ionization detector), an autosampler, and a capillary column (Rxi-  
255    5ms, 30 m × 0.32 mm internal diameter × 0.25 μm film thickness) were used. Helium (99.99%)  
256    was used as carrier gas at a constant flow rate of 1.2 mL.min<sup>-1</sup>. The temperature of the injector  
257    and the detector was set at 270 °C. The oven temperature was programmed as 35 °C (3 min)-  
258    15 °C.min<sup>-1</sup>-300°C. The injection volume was 5 μL, and the split ratio was 30:1. The standard  
259    deviation of analytical measurement was found to be lower than 0.70% indicating the high  
260    repeatability of the analysis.

261

### 262 3. RESULTS AND DISCUSSION

#### 263 3.1 Determination of reaction enthalpies

264

265 The mechanism for hydrogenation of alkyl levulinates to GVL is a two-step reaction (Scheme 1).  
266 The first step is hydrogenation of the carbonyl group to the intermediate (MHP or BHP). The  
267 second step is the cyclization of the intermediate to GVL. Based on this mechanism, one needs  
268 to evaluate/measure the two reaction enthalpies. In this study, both reaction enthalpies were  
269 calculated. GVL was used as a solvent for these experiments because BL and ML are soluble in  
270 GVL (Wang et al., 2019). The other benefit of GVL is its low vapor pressure value, e.g.,  $9.21 \times 10^{-4}$   
271 bar at 92.11°C, allowing to work at higher temperatures (Pokorny et al., 2017).

272

273 The reaction enthalpies  $\Delta H_{R,1}$  was defined as the amount of energy released/consumed by the  
274 hydrogenation reaction per mole of alkyl levulinate consumed, and  $\Delta H_{R,2}$  as the amount of energy  
275 released/consumed by the cyclization reaction per mole of GVL produced. The heat release in  
276 RC1 ( $Q_{RC1}$ ) includes the heat release from step 1 ( $Q_1$ ) and step 2 ( $Q_2$ ) as these two steps occur  
277 consecutively. In calorimeter C80, it is possible to measure only the heat of reaction 2 in the  
278 absence of hydrogen and Ru/C catalyst. The energy equations are shown below:

$$Q_{RC1} = \int_{t=0}^t (-R_1 \times V \times \Delta H_1 - R_2 \times V \times \Delta H_2) . dt = Q_1 + Q_2 \quad (1)$$

$$Q_{C80} = \int_{t=0}^t (-R_2 \times V \times \Delta H_2) . dt = Q_2 \quad (2)$$

279 where,  $Q_1$  and  $Q_2$  represent the heat of reactions 1 and 2, respectively;  $R_1$  and  $R_2$  represent the  
280 reaction rates 1 and 2;  $\Delta H_1$  and  $\Delta H_2$  represent the reaction enthalpies 1 and 2, respectively.

281

282

283

284 Instead of measuring the reaction rates, one can consider the material balance for the substrate:

$$n_{Subs,0} = n_{Subs}(t) + n_{Int}(t) + n_{GVL}(t) - n_{GVL,0} \quad (3)$$

285 The heat release from step 1 ( $Q_1$ ) depends on the first reaction enthalpy and mole conversion of  
286 substrate ML or BL (Eq. 4). The heat release of  $Q_2$  depends on the second reaction enthalpy and  
287 conversion of the intermediate to GVL (Eq. 5).

$$Q_1 = -(n_{Subs,0} - n_{Subs,final}) \times \Delta H_{R,1} \quad (4)$$

$$Q_2 = +(n_{GVL,0} - n_{GVL,final}) \times \Delta H_{R,2} \quad (5)$$

288 From Eqs (1) and (2), one can obtain the equations for the calculation of reaction enthalpy:

$$\Delta H_{R,2} = \frac{+Q_{C80}}{n_{GVL,0} - n_{GVL,final}} \quad (6)$$

$$\Delta H_{R,1} = \frac{Q_{RC1} - (n_{GVL,0} - n_{GVL,final}) \times \Delta H_{R,2}}{-(n_{Subs,0} - n_{Subs,final})} \quad (7)$$

289

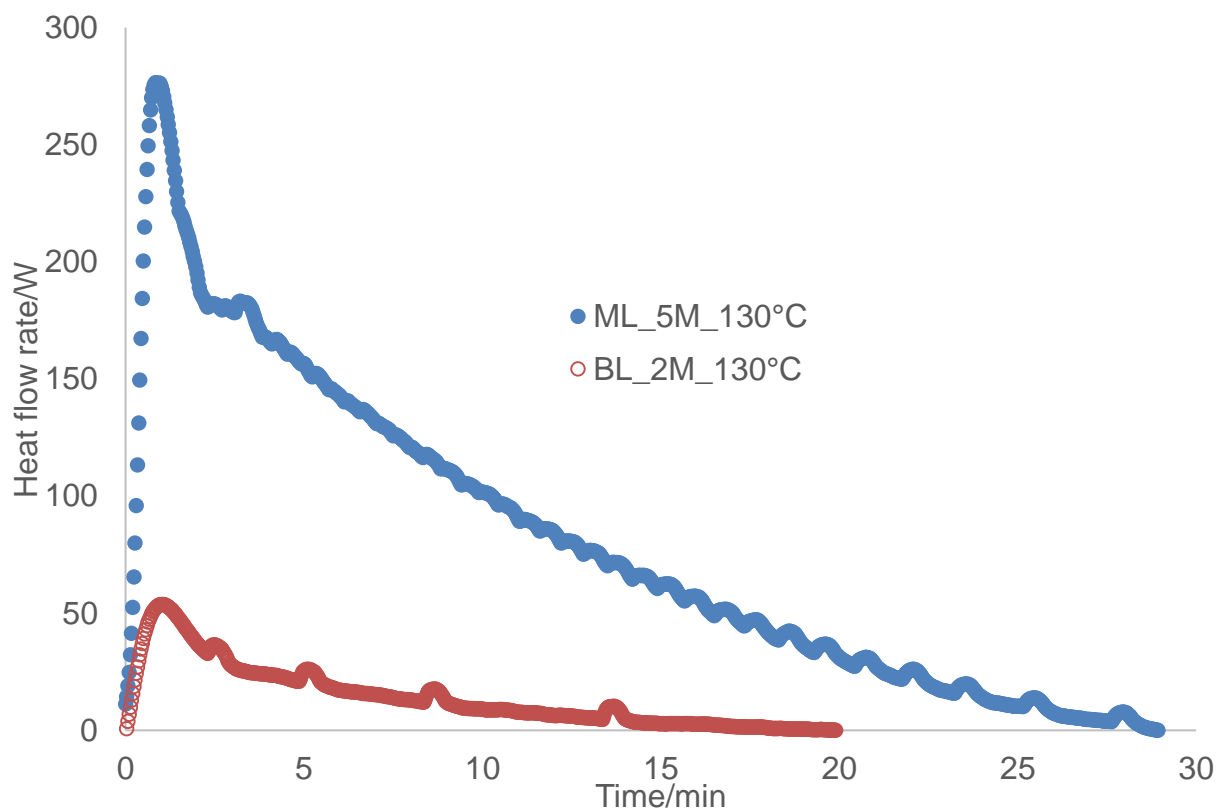
290 As in C80 experiment, only step 2 occurs so the reaction enthalpy for the second step ( $\Delta H_{R,2}$ ) can  
291 be calculated firstly. Then by using the value of  $\Delta H_{R,2}$ , the reaction enthalpy for the first reaction  
292 ( $\Delta H_{R,1}$ ) can be obtained.

293

### 294 3.1.1 RC1 results

295 Fig. 3 shows the evolution of the heat flow rate released by the reactions for the hydrogenation of  
296 ML and BL under isothermal conditions at 130°C. The time zero was set when the stirring was  
297 started.

298



299

300 Fig. 3 - Heat flow rate for hydrogenation of ML and BL to GVL in RC1 under isothermal  
 301 conditions at 130°C.

302

303 By integrating the peak area from time 0 to the end of the experiment, the total energy released  
 304 ( $Q_{RC1}$ ) from this reaction can be obtained (Table 4).

305

306 Table 4. GC and RC1 results for experiments under isothermal condition.

	Initial concentration (mol/L)		Final concentration (mol/L)			$Q_{RC1}$ (kJ)
	Substrate	GVL	Substrate	GVL	Intermediate	
ML	5.15	3.9	0.00	5.16	3.40	+158.26
BL	2.04	6.79	0.44	7.26	0.79	+34.187

307

308

309

310 The reaction mixture before and after experiments were analyzed by GC (Table 4). From the  
311 material balance analysis, no side reactions were noticed. The conversion of ML was total but not  
312 the conversion of MHP to GVL. One can notice that the kinetics for the BL system was slower.  
313 Globally, these reaction systems are exothermic, and the total energy released per GVL produced  
314 by the ML system is higher than for the BL system in absolute value (Table 6).

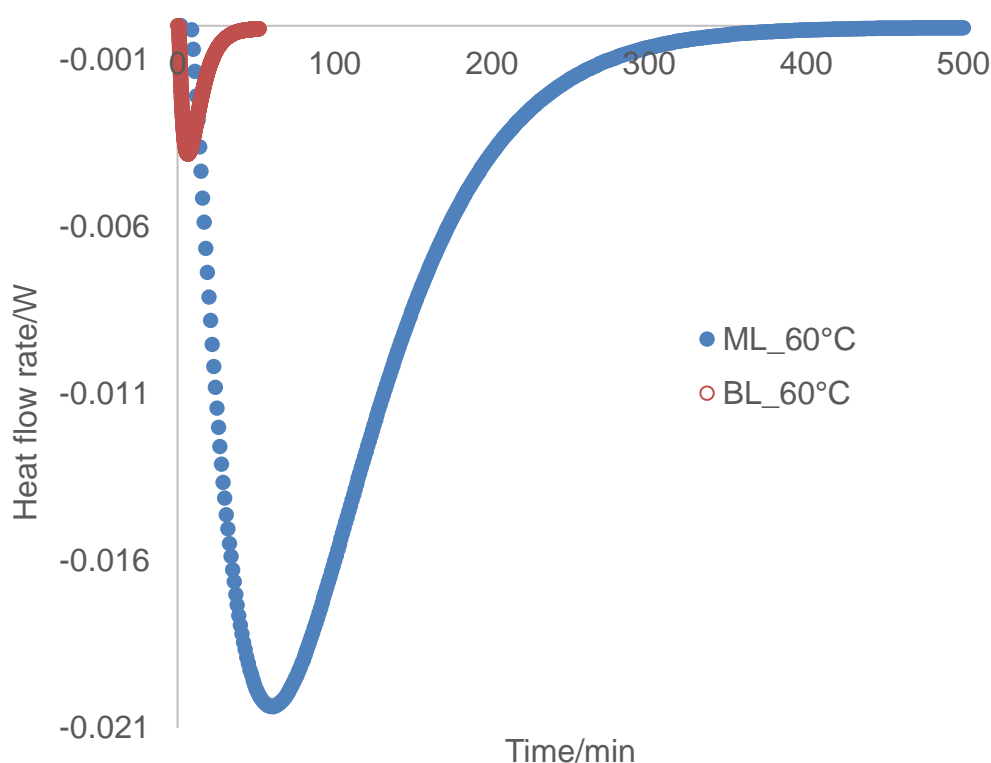
315

### 316 3.1.2 C80 results

317 Before the C80 rotation in measurement cell, the reaction mixture in the open tube comprised  
318 substrates, intermediates, alcohols and GVL; and the outside container comprised GVL and  
319 sulfuric acid to catalyze the cyclization reaction. The time zero is when the C80 starts to rotate.

320 The cyclization reaction is endothermic as illustrated by Fig. 4.

321



322

323 Fig. 4 - Heat flow rate profiles for the cyclization reaction of MHP and BHP in C80 at 60°C.

324

325 By integrating the heat flow rate peak, the total energy absorbed by the reaction can be calculated.

326 Table 5 shows the results of the C80 calorimeter.

327 Table 5. GC and C80 experiments.

	Initial concentration (mol/L)			Final concentration (mol/L)			Q <sub>C80</sub> (kJ)
	Substrate	GVL	Intermediate	Substrate	GVL	Intermediate	
ML	0.00	7.80	1.70	0.00	8.99	0.41	-0.018
BL	0.17	9.01	0.33	0.17	9.48	0.03	-0.004

328

329 From Table 5, one can notice that the energy absorbed by the second reaction is slightly higher  
330 for the MHP cyclization than for the BHP cyclization. The reaction enthalpy 2 for ML system is  
331 +7 kJ/mol, and for BL system is +6.5 kJ/mol.

332 From Eq. (7), one can find that the values of reaction enthalpy 1 for ML is -53.25 kJ/mol and -  
333 38.66 kJ/mol for BL. Table 6 summarizes the different reaction enthalpy.

334

335 One can conclude that reaction 1, i.e., hydrogenation, governs the reaction temperature of this  
336 system. The hydrogenation enthalpy for the ML system is higher than the one for the BL system.  
337 This observation shows that the substituent plays a role not only on the kinetics (Wang et al., 2019)  
338 but also on the thermodynamics.

339

340 Table 6. Reaction enthalpies for each step in the GVL solvent.

	ML	BL
$\Delta H_{R,1}$	-53.25 kJ/mol	-38.66 kJ/mol
$\Delta H_{R,2}$	+7.00 kJ/mol	+6.50 kJ/mol

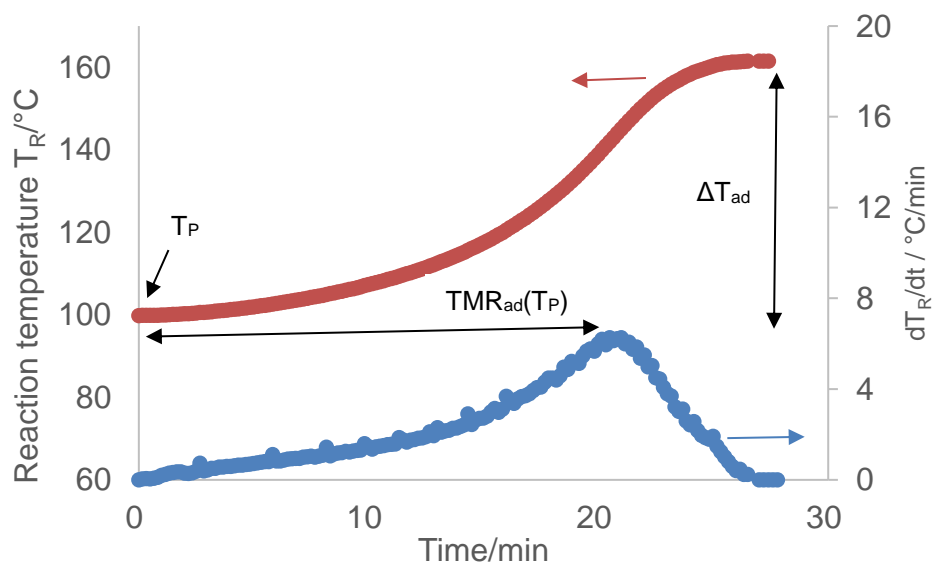
341

342

343 **3.2 Thermal risk assessment**

344 The aim of this section is not to develop a detailed kinetic model based on adiabatic experiments  
345 but to calculate various thermal risk parameters such as  $T_{D24}$ ,  $T_{D8}$ ,  $TMR_{ad}(T_p)$ , and  $\Delta T_{ad}$  as  
346 accurately as possible instead of the zero-order model (Vernières-Hassimi et al., 2017).

347 The parameter  $TMR_{ad}(T_p)$  is the time to reach the maximum rate from the initial temperature  $T_p$ ,  
348 and is obtained from the derivative of the reaction temperature. The parameters  $T_{D24}$  and  $T_{D8}$  are  
349 the initial temperatures to get  $TMR_{ad}$  of 24 and 8 hours, respectively. The parameter  $\Delta T_{ad}$   
350 corresponds to the difference between the final and initial temperatures. For the sake of clarity,  
351 Fig. 5 illustrates the values of these parameters.



352

353 Fig. 5 – Thermal risk parameters under adiabatic conditions.

354 As already noted, it is the hydrogenation reaction that determines the reaction temperature, since  
355 the second enthalpy of the reaction is very low. Therefore, this second reaction can be neglected  
356 for the kinetic model under adiabatic conditions, and the reaction rate takes the following form:

357 
$$R_1 = k_1 \times [Substrate]_{liq} \times P_{H_2} \times \omega_{Cat}. \quad (8)$$

358 As it was observed in the previous study of our group (Wang et al., 2019), the kinetics of hydrogen  
 359 mass transfer is faster than the ones of the chemical reaction. Hence, the concentration of  
 360 hydrogen in the bulk liquid phase is assumed to be the same as the one at the gas-liquid interface.  
 361 The material balance equations for substrate and intermediate in the autoclave are then simply  
 362 represented as:

$$363 \quad \frac{d[\text{substrate}]}{dt} = -R_1 \quad (9)$$

$$364 \quad \frac{d[\text{intermediate}]}{dt} = R_1 \quad (10)$$

365 while the heat balance equation for the liquid phase is:

$$366 \quad \frac{dT_R}{dt} = \frac{-R_1 \times \Delta H_{R1} \times V}{m_R \times C_{PR} + m_{\text{insert}} \times C_{p\text{insert}}} \quad (11)$$

367

368 The term  $m_R \times C_{PR}$  was evaluated by  $m_R \times (w_{\text{subs},0} \times C_{p\text{subs}}(T_R) + w_{\text{GVL},0} \times C_{p\text{GVL}}(T_R))$ ,  
 369 where  $w_{\text{subs},0}$  and  $w_{\text{GVL},0}$  are the initial mass fraction of the substrates and GVL. The variation of  
 370 the specific heat capacity with temperature was taken into account. According to the manufacturer,  
 371 the term heat capacity of the insert is 52 J/K.

372

373 A modified Arrhenius equation was used to decrease the correlation between the pre-exponential  
 374 factor and activation energy:

$$375 \quad k_1(T) = k_1(T_{\text{Ref}}) \times \exp\left(\frac{-Ea}{R} \times \left(\frac{1}{T} - \frac{1}{T_{\text{Ref}}}\right)\right) \quad (12)$$

376 As mentioned, reaction temperatures and the hydrogen pressures in the autoclave were monitored  
 377 online during the hydrogenation process.

378 Based on the standard least-squares method, the predictions of developed model equations (Eqs  
 379 8-12) with appropriate boundary conditions were then fitted to the online measured reaction  
 380 temperature, where the rate constants at a reference temperature ( $T_{ref}$ ) and activation energies  
 381 served as fitting parameters.

382

383 The software ModEst was used to estimate the kinetic constant of the first reaction for the ML  
 384 and BL system (Haario, 1994). ODESSA, which uses the backward difference method, solved the  
 385 ordinary differential equations. A Levenberg-Marquardt algorithm was used to optimize the  
 386 objective function, defined as

$$387 \quad \omega = \sum_i (y_i - \hat{y}_i)^2 \quad (13)$$

388 where,  $y_i$  is the experimental reaction temperature value and  $\hat{y}_i$  is the simulated one.

389

390 Fig. 6 shows the fit of the model to the experimental temperature. One can conclude that the  
 391 model can predict the temperature evolution. Table 7 displays the values of the estimated  
 392 parameters and the standard deviation. The values of the standard deviation are very low. However,  
 393 there is a strong correlation between the rate constant at 130°C and the activation energy, i.e.,  
 394 0.992. This strong correlation might be due to the simplified kinetic model used.

395 Table 7. Estimated kinetic constants and standard deviation at  $T_{Ref}=130^\circ\text{C}$  for the ML system.

	Units	Estimated parameters	Relative standard deviation (%)
$k_1(T_{Ref})$	L/(bar.kg_dry basis_cat.s)	$0.535 \times 10^{-08}$	0.7
$Ea_1$	J/mol	$0.822 \times 10^{+05}$	0.6

396

397 The coefficient of determination was found to be equal to 98.92% for the modeling of BL  
 398 hydrogenation under adiabatic mode. Fig. 6 shows the fit of the model to the experimental  
 399 temperature. One can conclude that the model can predict the temperature evolution. Table 8  
 400 displays the values of the estimated parameters and the standard deviation. The values of the  
 401 standard deviation are very low. However, there is a strong correlation between the rate constant  
 402 at 130°C and the activation energy, i.e., 0.998.

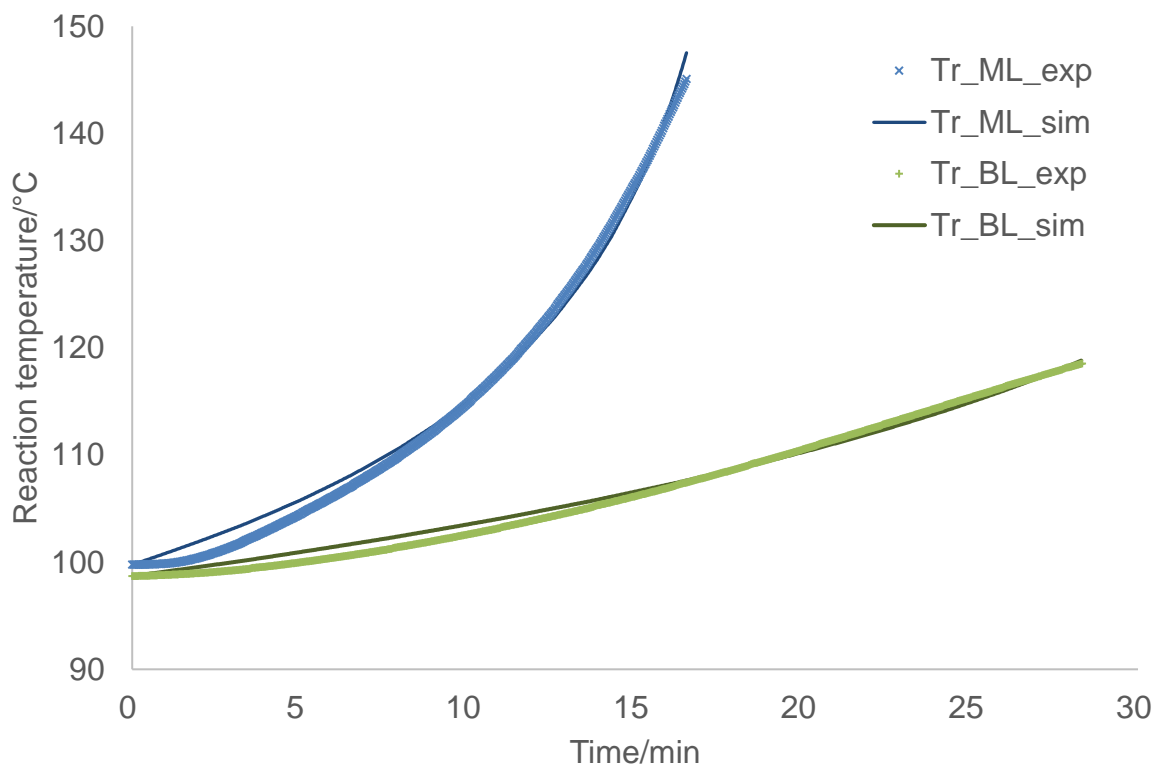
403 Table 8. Estimated kinetic constants and standard deviation at  $T_{Ref}=130^{\circ}C$  for the BL system.

	Units	Estimated parameters	Relative standard deviation (%)
$k_1(T_{Ref})$	L/(bar.kg_dry basis_cat.s)	$0.350 \times 10^{-08}$	2.3
$Ea_1$	J/mol	$0.857 \times 10^{+05}$	1.3

404

405

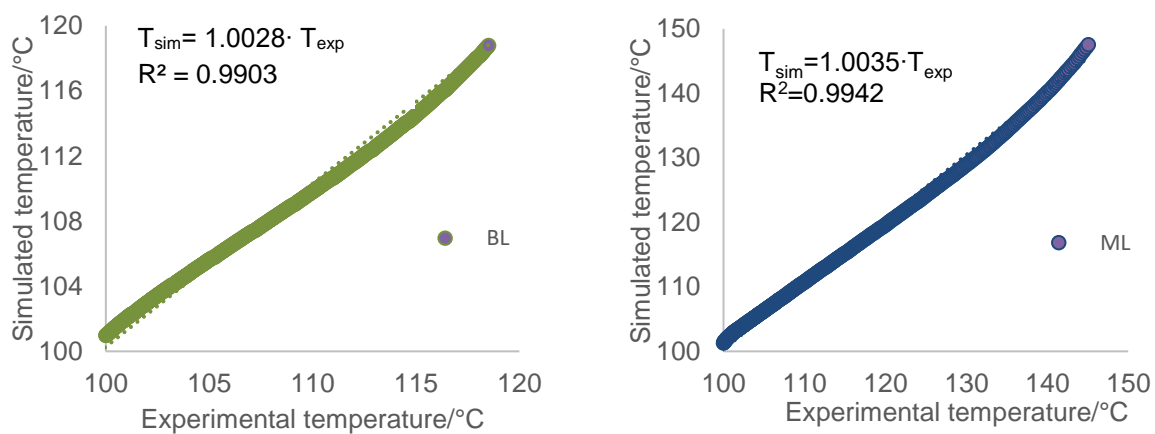
406



407

408 Fig. 6 - Temperature profiles for the hydrogenation of BL and ML under adiabatic conditions.

409 Figs 7 show the high reliability of both models.



410

411 Fig. 7 - Overall parity plots of experimental temperature versus simulated temperatures for BL  
412 and ML systems.

413

414 One can notice that the kinetics of ML hydrogenation is faster than BL hydrogenation, as it was  
415 demonstrated in previous articles (Negahdar et al., 2017; Wang et al., 2019). Based on this model,  
416 it is possible to estimate different thermal risk parameters under the same operating conditions as  
417 described in Table 9.

418 Table 9. Thermal risk parameters for the hydrogenation of ML and BL.

	$T_{D24}$ (°C)	$T_{D8}$ (°C)	$TMR_{ad}(100^{\circ}C)$ (hrs)	$\Delta T_{ad}$ (°C)
Hydrogenation of ML	49	62	0.55	66
Hydrogenation of BL	60	74	1.20	47

419

420 By using the criteria defined in the article by Wang et al. (2018), both reaction systems present a  
421 medium thermal risk with the operating conditions of Table 2. Even if for BL system, the  
422  $TMR_{ad}(100^{\circ}C)$  value gives a probable risk and  $\Delta T_{ad}$  value gives a medium severity, one should  
423 keep in mind that this reaction system is under hydrogen pressure.

424 Further information can be provided by calculating the values of  $T_{D24}$  and  $T_{D8}$ . These parameters  
425 represent the initial temperature under adiabatic mode to reach the fastest temperature rate in 24  
426 hours and 8 hours. One should notice that the values of these parameters are lower than  $100^{\circ}C$ .  
427 The classical temperature for this reaction system can be up to  $160^{\circ}C$  under isothermal conditions.  
428 Hence, safety barriers, such as an additional cooling system, must be added in the case of thermal  
429 runaway.

430

#### 431        **4. CONCLUSIONS**

432        In this study, thermal risk assessment for the production of  $\gamma$ -valerolactone (GVL) from the  
433        hydrogenation of methyl levulinate (ML) and butyl levulinate (BL) over Ru/C was carried out.  
434        To achieve this goal, the reaction enthalpies were measured, and kinetic models were developed  
435        based on experiments performed under adiabatic conditions. For that, two types of calorimeters  
436        were used: Mettler Toledo RC1 and Setaram Tian-Calvet C80.

437        Hydrogenation of alkyl levulinates over Ru/C is a two-step reaction: hydrogenation and  
438        cyclization. It was experimentally found that the overall reaction is exothermic. The  
439        hydrogenation reaction enthalpy was calculated to be -53.25 kJ/mol for the ML hydrogenation  
440        and -38.66 kJ/mol for the BL hydrogenation. These values confirm the exothermic behavior of  
441        the first reaction step. The cyclization reaction enthalpy was measured to be +7 kJ/mol for the  
442        ML system and +6.5 kJ/mol for the BL system. These values show that this second reaction step  
443        is endothermic, and it is negligible compared to the hydrogenation step.

444        Adiabatic experiments in RC1 calorimeter were performed with the following operating  
445        conditions: initial substrate concentration of ca. 4.5 mol/L, dry basis catalyst loading of  $5.4 \times 10^{-3}$   
446        kg/L, and initial reaction temperature of 100°C. It was found that the thermal risk for both systems  
447        can be considered as a medium for such operating conditions based on  $TMR_{ad}$  and  $\Delta T_{ad}$ . Safety  
448        barriers must be implemented for such a reaction system to decrease the risk of thermal runaway.  
449        A further investigation is to evaluate the optimum operating conditions to find a compromise  
450        between safety and productivity.

451

452 **ACKNOWLEDGEMENTS**

453 This study has been done in the framework of Task 2: “Green process: 2<sup>nd</sup> generation of biomass”  
454 of AMED project. The authors thank the AMED project. The AMED project has been funded with  
455 the support from the European Union with the European Regional Development Fund (ERDF)  
456 and from the Regional Council of Normandie. The China Scholarship Council: Cooperation  
457 Program with the UTs and INSAs (France) is thanked by the authors. The authors also thank the  
458 PHC program Proteus “Process intensification in the production of 2<sup>nd</sup> generation platform  
459 molecules” (41657WB). The authors thank Jean-Pierre Hébert for his huge help for the  
460 experimental part with the Mettler Toledo RC1.

461

462 **NOMENCLATURE**

$C_p$	Specific heat-capacity [J/(kg.K)]
$E_a$	Activation energy [J/mol]
$\Delta H_R$	Reaction enthalpy [J/mol]
$k$	Rate constant
$V_{liq}$	Volume of liquid [L]
$m_{insert}$	Insert mass [kg]
$P$	Pressure [bar]
$R$	Gas constant [J/(K.mol)]
$R^2$	Coefficient of determination [%]
$\Delta T_{ad}$	Adiabatic temperature rise [°C]
$T_R$	Temperature of the reaction mixture [°C]
$T_{Ref}$	Reference temperature [°C]
$R_i$	reaction rate $i$ [mol/(L.s)]
$w_i$	weight percent
$y_i$	experimental observable
$\bar{y}$	mean value of the experimental observables
$\hat{y}_i$	observable simulated by the model

463

464 **Greek letters**

$\omega$	Objective function
$\omega_{cat.}$	catalyst loading [kg/L]

465

466

467

468 **Subscripts and superscripts**

Ref reference

\* interfacial value

469

470 **Abbreviations**

BL butyl levulinate

BHP n-butyl 4-hydroxypentanoate

GVL  $\gamma$ -valerolactone

ML methyl levulinate

MHP methyl 4-hydroxypentanoate

ROH co-product of the second reaction (methanol or butanol)

TMR<sub>ad</sub> Time-to-maximum rate under adiabatic conditions at T<sub>P</sub> [hrs]

471

472

473

474 **REFERENCES**

- 475 Al-Naji, M., Puértolas, B., Kumru, B., Cruz, D., Bäümel, M., Schmidt, B.V.K.J., Tarakina, N.V.,  
476 Pérez-Ramírez, J., 2019. Sustainable continuous flow valorization of  $\gamma$ -valerolactone with  
477 trioxane to  $\alpha$ -methylene- $\gamma$ -valerolactone over basic beta zeolites. *ChemSusChem* 12, 2628–2636.  
478 <https://doi.org/10.1002/cssc.201900418>
- 479 Alonso, D.M., Wettstein, S.G., Mellmer, M.A., Gurbuz, E.I., Dumesic, J.A., 2012. Integrated  
480 conversion of hemicellulose and cellulose from lignocellulosic biomass. *Energy Environ. Sci.* 6,  
481 76–80. <https://doi.org/10.1039/C2EE23617F>
- 482 Al-Shaal, M.G., Calin, M., Delidovich, I., Palkovits, R., 2016. Microwave-assisted reduction of  
483 levulinic acid with alcohols producing  $\gamma$ -valerolactone in the presence of a Ru/C catalyst. *Catal.*  
484 *Commun.* 75, 65–68. <https://doi.org/10.1016/j.catcom.2015.12.001>
- 485 An, R., Xu, G., Chang, C., Bai, J., Fang, S., 2017. Efficient one-pot synthesis of n-butyl levulinate  
486 from carbohydrates catalyzed by  $\text{Fe}_2(\text{SO}_4)_3$ . *J. Energy Chem.* 26, 556–563.  
487 <https://doi.org/10.1016/j.jechem.2016.11.015>
- 488 Bollyn, M., 2006. DMSO can be more than a solvent: thermal analysis of its chemical interactions  
489 with certain chemicals at different process stages. *Org. Process Res. Dev.* 10, 1299–1312.  
490 <https://doi.org/10.1021/op060158p>
- 491 Bond, J.Q., Alonso, D.M., Wang, D., West, R.M., Dumesic, J.A., 2010. Integrated catalytic  
492 conversion of  $\gamma$ -valerolactone to liquid alkenes for transportation fuels. *Science* 327, 1110–1114.  
493 <https://doi.org/10.1126/science.1184362>
- 494 Borregaard, 2019. Capacity increase for bio-based vanillin.  
495 <https://www.borregaard.com/News/Capacity-increase-for-bio-based-vanillin> (accessed 3 July  
496 2020).
- 497 Bourne, R.A., Stevens, J.G., Ke, J., Poliakoff, M., 2007. Maximising opportunities in supercritical  
498 chemistry: the continuous conversion of levulinic acid to  $\gamma$ -valerolactone in  $\text{CO}_2$ . *Chem.*

499 Commun. 4632–4634. <https://doi.org/10.1039/B708754C>

500 Bozell, J.J., Moens, L., Elliott, D.C., Wang, Y., Neuenschwander, G.G., Fitzpatrick, S.W., Bilski,  
501 R.J., Jarnefeld, J.L., 2000. Production of levulinic acid and use as a platform chemical for derived  
502 products. *Resour. Conserv. Recy.* 28, 227–239. [https://doi.org/10.1016/S0921-3449\(99\)00047-6](https://doi.org/10.1016/S0921-3449(99)00047-6)

503 Brown, D.B., Ironside, M.D., Shaw, S.M., 2016. Safety notables: Information from the literature.  
504 *Org. Process Res. Dev.* 20, 575–582. <https://doi.org/10.1021/acs.oprd.6b00013>

505 Budzianowski, W.M., Postawa, K., 2016. Total Chain Integration of sustainable biorefinery  
506 systems. *Appl. Energy* 184, 1432–1446. <https://doi.org/10.1016/j.apenergy.2016.06.050>

507 Casson Moreno, V., Cozzani, V., 2015. Major accident hazard in bioenergy production. *J. Loss  
508 Prevent. Proc.* 35, 135–144. <https://doi.org/10.1016/j.jlp.2015.04.004>

509 Casson Moreno, V., Garbetti, A.L., Leveneur, S., Antonioni, G., 2019. A consequences-based  
510 approach for the selection of relevant accident scenarios in emerging technologies. *Saf. Sci.* 112,  
511 142–151. <https://doi.org/10.1016/j.ssci.2018.10.024>

512 Casson Moreno, V., Papasidero, S., Scarponi, G.E., Guglielmi, D., Cozzani, V., 2016. Analysis  
513 of accidents in biogas production and upgrading. *Renew. Energy* 96, 1127–1134.  
514 <https://doi.org/10.1016/j.renene.2015.10.017>

515 Chandel, A.K., Garlapati, V.K., Kumar, S.P.J., Hans, M., Singh, A.K., Kumar, S., n.d. The role  
516 of renewable chemicals and biofuels in building a bioeconomy. *Biofuel Bioprod. Biorefin.* n/a.  
517 <https://doi.org/10.1002/bbb.2104>

518 Chew, A.K., Walker, T.W., Shen, Z., Demir, B., Witteman, L., Euclide, J., Huber, G.W.,  
519 Dumesic, J.A., Van Lehn, R.C., 2020. Effect of mixed-solvent environments on the selectivity of  
520 acid-catalyzed dehydration reactions. *ACS Catal.* 10, 1679–1691.  
521 <https://doi.org/10.1021/acscatal.9b03460>

522 Chi, J.-H., Wu, S.-H., Shu, C.-M., 2009. Thermal explosion analysis of methyl ethyl ketone  
523 peroxide by non-isothermal and isothermal calorimetric applications. *J. Hazard. Mater.* 171,

524 1145–1149. <https://doi.org/10.1016/j.jhazmat.2009.06.125>

525 Dakkoune, A., Vernières-Hassimi, L., Leveneur, S., Lefebvre, D., Estel, L., 2018. Risk analysis  
526 of French chemical industry. *Saf. Sci.* 105, 77–85. <https://doi.org/10.1016/j.ssci.2018.02.003>

527 Delhaye, L., Stevens, C., Merschaert, A., Delbeke, P., Briône, W., Tilstam, U., Borghese, A.,  
528 Geldhof, G., Diker, K., Dubois, A., Barberis, M., Casarubios, L., 2007. Development of a scalable  
529 process for the synthesis of trans-2-methylcyclopropanecarboxylic acid. *Org. Process Res. Dev.*  
530 11, 1104–1111. <https://doi.org/10.1021/op600275g>

531 di Bitonto, L., Antonopoulou, G., Braguglia, C., Campanale, C., Gallipoli, A., Lyberatos, G.,  
532 Ntaikou, I., Pastore, C., 2018. Lewis-Brønsted acid catalysed ethanolysis of the organic fraction  
533 of municipal solid waste for efficient production of biofuels. *Bioresour. Technol.* 266, 297–305.  
534 <https://doi.org/10.1016/j.biortech.2018.06.110>

535 Ding, D., Xi, J., Wang, J., Liu, X., Lu, G., Wang, Y., 2015. Production of methyl levulinate from  
536 cellulose: selectivity and mechanism study. *Green Chem.* 17, 4037–4044.  
537 <https://doi.org/10.1039/C5GC00440C>

538 Dockerty, T., Appleton, K., Lovett, A., 2012. Public opinion on energy crops in the landscape:  
539 considerations for the expansion of renewable energy from biomass. *J. Environ. Plan. Manag.* 55,  
540 1134–1158. <https://doi.org/10.1080/09640568.2011.636966>

541 Dong, Z., Chen, L., Ma, Y., Peng, H., Chen, W., 2018. Adiabatic correction for the esterification  
542 of acetic anhydride by methanol via accurate kinetics. *Chin. J. Chem. Eng.* 26, 1954–1959.  
543 <https://doi.org/10.1016/j.cjche.2017.10.005>

544 Dutta, S., Yu, I.K.M., Tsang, D.C.W., Ng, Y.H., Ok, Y.S., Sherwood, J., Clark, J.H., 2019. Green  
545 synthesis of gamma-valerolactone (GVL) through hydrogenation of biomass-derived levulinic  
546 acid using non-noble metal catalysts: A critical review. *Chem. Eng. J.* 372, 992–1006.  
547 <https://doi.org/10.1016/j.cej.2019.04.199>

548 Feng, X., Tian, Y., Xiao, L., Wu, W., 2020. Fe–Mo<sub>2</sub>C: A magnetically recoverable catalyst for

549 hydrogenation of ethyl levulinate into  $\gamma$ -valerolactone. Catal Lett.  
550 <https://doi.org/10.1007/s10562-020-03124-z>

551 Gallezot, P., 2012. Conversion of biomass to selected chemical products. Chem. Soc. Rev. 41,  
552 1538–1558. <https://doi.org/10.1039/C1CS15147A>

553 Gigante, L., Lunghi, A., Martinelli, S., Cardillo, P., Picello, L., Bortolaso, R., Galvagni, M., Rota,  
554 R., 2003. Calorimetric approach and simulation for scale-up of a Friedel–Crafts reaction. Org.  
555 Process Res. Dev. 7, 1079–1082. <https://doi.org/10.1021/op030043a>

556 Girgis, M.J., Kiss, K., Ziltener, C.A., Prashad, M., Har, D., Yoskowitz, R.S., Basso, B., Repic,  
557 O., Blacklock, T.J., Landau, R.N., 1997. Kinetic and calorimetric considerations in the scale-up  
558 of the catalytic reduction of a substituted nitrobenzene. Org. Process Res. Dev. 1, 339–349.  
559 <https://doi.org/10.1021/op970015q>

560 Golikova, A., Tsvetov, N., Samarov, A., Toikka, M., Zvereva, I., Trofimova, M., Toikka, A.,  
561 2020. Excess enthalpies and heat of esterification reaction in ethanol + acetic acid + ethyl  
562 acetate + water system at 313.15 K. J. Therm. Anal. Calorim. 139, 1301–1307.  
563 <https://doi.org/10.1007/s10973-019-08488-y>

564 GranBio, 2014. GranBio begins producing second-generation ethanol. [http://news.bio-](http://news.bio-based.eu/granbio-begins-producing-second-generation-ethanol/)  
565 [based.eu/granbio-begins-producing-second-generation-ethanol/](http://news.bio-based.eu/granbio-begins-producing-second-generation-ethanol/) (accessed 3 July 2020).

566 Haario, H., 2001. MODEST-User’s Guide, in: Profmath Oy, Helsinki.

567 Hayes, D. J., Fitzpatrick, S., Hayes, M. H. B, Ross, J. R. H., 2005. The Biofine Process –  
568 Production of Levulinic Acid, Furfural, and Formic Acid from Lignocellulosic Feedstocks, in  
569 Biorefineries-Industrial Processes and Products: Status Quo and Future Directions, in: Kamm, B.,  
570 Gruber, P. R., Kamm, M. (Eds.), Wiley-VCH Verlag GmbH, Weinheim.

571 Hoffmann, W., Kang, Y., Mitchell, J.C., Snowden, M.J., 2007. Kinetic data by nonisothermal  
572 reaction calorimetry: a model-assisted calorimetric evaluation. Org. Process Res. Dev. 11, 25–  
573 29. <https://doi.org/10.1021/op060144j>

574 Horváth, I.T., Mehdi, H., Fábos, V., Boda, L., Mika, L.T., 2008.  $\gamma$ -valerolactone—a sustainable  
575 liquid for energy and carbon-based chemicals. *Green Chem.* 10, 238–242.  
576 <https://doi.org/10.1039/B712863K>

577 Huber, G.W., Iborra, S., Corma, A., 2006. Synthesis of transportation fuels from biomass:  
578 chemistry, catalysts, and engineering. *Chem. Rev.* 106, 4044–4098.  
579 <https://doi.org/10.1021/cr068360d>

580 Jhu, C.-Y., Wang, Y.-W., Wen, C.-Y., Shu, C.-M., 2012. Thermal runaway potential of  $\text{LiCoO}_2$   
581 and  $\text{Li}(\text{Ni}_{1/3}\text{Co}_{1/3}\text{Mn}_{1/3})\text{O}_2$  batteries determined with adiabatic calorimetry methodology.  
582 *Applied Energy, Clean Energy for Future Generations* 100, 127–131.  
583 <https://doi.org/10.1016/j.apenergy.2012.05.064>

584 Kortsch, T., Hildebrand, J., Schweizer-Ries, P., 2015. Acceptance of biomass plants – Results of  
585 a longitudinal study in the bioenergy-region Altmark. *Renew. Energy* 83, 690–697.  
586 <https://doi.org/10.1016/j.renene.2015.04.059>

587 Leveneur, S., 2017. Thermal safety assessment through the concept of structure–reactivity:  
588 application to vegetable oil valorization. *Org. Process Res. Dev.* 21, 543–550.  
589 <https://doi.org/10.1021/acs.oprd.6b00405>

590 Leveneur, S., Pinchard, M., Rimbault, A., Safdari Shadloo, M., Meyer, T., 2018. Parameters  
591 affecting thermal risk through a kinetic model under adiabatic condition: Application to liquid-  
592 liquid reaction system. *Thermochim. Acta* 666, 10–17. <https://doi.org/10.1016/j.tca.2018.05.024>

593 Leveneur, S., Vernieres-Hassimi, L., Salmi, T., 2016. Mass & energy balances coupling in  
594 chemical reactors for a better understanding of thermal safety. *Educ. Chem. Eng.* 16, 17–28.  
595 <https://doi.org/10.1016/j.ece.2016.06.002>

596 Li, F., Li, Z., France, L.J., Mu, J., Song, C., Chen, Y., Jiang, L., Long, J., Li, X., 2018. Highly  
597 efficient transfer hydrogenation of levulinate esters to  $\gamma$ -valerolactone over basic zirconium  
598 carbonate. *Ind. Eng. Chem. Res.* 57, 10126–10136. <https://doi.org/10.1021/acs.iecr.8b00712>

599 Lin, H., Chen, J., Zhao, Y., Wang, S., 2017. Conversion of C5 carbohydrates into furfural  
600 catalyzed by so3h-functionalized ionic liquid in renewable  $\gamma$ -valerolactone. *Energ. Fuels* 31,  
601 3929–3934. <https://doi.org/10.1021/acs.energyfuels.6b01975>

602 Liu, C., Wei, M., Wang, J., Xu, J., Jiang, J., Wang, K., 2020. Facile directional conversion of  
603 cellulose and bamboo meal wastes over low-cost sulfate and polar aprotic solvent. *ACS*  
604 *Sustainable Chem. Eng.* 8, 5776–5786. <https://doi.org/10.1021/acssuschemeng.0c01280>

605 Liu, S.H., Hou, H.Y., Chen, J.W., Weng, S.Y., Lin, Y.C., Shu, C.M., 2013. Effects of thermal  
606 runaway hazard for three organic peroxides conducted by acids and alkalines with DSC, VSP2,  
607 and TAM III. *Thermochim. Acta* 566, 226–232. <https://doi.org/10.1016/j.tca.2013.05.029>

608 Lunghi, A., Alós, M.A., Gigante, L., Feixas, J., Sironi, E., Feliu, J.A., Cardillo, P., 2002.  
609 Identification of the decomposition products in an industrial nitration process under thermal  
610 runaway conditions. *Org. Process Res. Dev.* 6, 926–932. <https://doi.org/10.1021/op0255884>

611 Luo, W., Deka, U., Beale, A.M., van Eck, E.R.H., Bruijninx, P.C.A., Weckhuysen, B.M., 2013.  
612 Ruthenium-catalyzed hydrogenation of levulinic acid: Influence of the support and solvent on  
613 catalyst selectivity and stability. *J. Catal.* 301, 175–186.  
614 <https://doi.org/10.1016/j.jcat.2013.02.003>

615 Luterbacher, J.S., Rand, J.M., Alonso, D.M., Han, J., Youngquist, J.T., Maravelias, C.T., Pfleger,  
616 B.F., Dumesic, J.A., 2014. Nonenzymatic sugar production from biomass using biomass-derived  
617  $\gamma$ -valerolactone. *Science* 343, 277–280. <https://doi.org/10.1126/science.1246748>

618 Maestri, F., Re Dionigi, L., Rota, R., Gigante, L., Lunghi, A., Cardillo, P., 2006. Safe and  
619 productive operation of homogeneous semibatch reactors. II. The nitration of N-(2-  
620 Phenoxyphenyl) methane sulfonamide. *Ind. Eng. Chem. Res.* 45, 8014–8023.  
621 <https://doi.org/10.1021/ie060262v>

622 Makhubela, B.C.E., Darkwa, J., 2018. The role of noble metal catalysts in conversion of biomass  
623 and bio-derived intermediates to fuels and chemicals. *Johnson Matthey Technology Review* 62,

624 4–31. <https://doi.org/10.1595/205651317X696261>

625 Marco, E., Cuartielles, S., Peña, J.A., Santamaria, J., 2000. Simulation of the decomposition of  
626 di-cumyl peroxide in an ARSST unit. *Thermochim. Acta* 362, 49–58.  
627 [https://doi.org/10.1016/S0040-6031\(00\)00587-6](https://doi.org/10.1016/S0040-6031(00)00587-6)

628 Mellmer, M.A., Alonso, D.M., Luterbacher, J.S., Gallo, J.M.R., Dumesic, J.A., 2014. Effects of  
629  $\gamma$ -valerolactone in hydrolysis of lignocellulosic biomass to monosaccharides. *Green Chem.* 16,  
630 4659–4662. <https://doi.org/10.1039/C4GC01768D>

631 Negahdar, L., Al-Shaal, M.G., Holzhäuser, F.J., Palkovits, R., 2017. Kinetic analysis of the  
632 catalytic hydrogenation of alkyl levulinates to  $\gamma$ -valerolactone. *Chem. Eng. Sci.* 158, 545–551.  
633 <https://doi.org/10.1016/j.ces.2016.11.007>

634 Peng, L., Lin, L., Zhang, J., Shi, J., Liu, S., 2011. Solid acid catalyzed glucose conversion to ethyl  
635 levulinate. *Appl. Catal. A-Gen.* 397, 259–265. <https://doi.org/10.1016/j.apcata.2011.03.008>

636 Pérez-Sena, W.Y., Salmi, T., Estel, L., Leveneur, S., 2020. Thermal risk assessment for the  
637 epoxidation of linseed oil by classical Prileschajew epoxidation and by direct epoxidation by  
638  $H_2O_2$  on alumina. *J. Therm. Anal. Calorim.* 140, 673–684. [https://doi.org/10.1007/s10973-019-](https://doi.org/10.1007/s10973-019-08894-2)  
639 08894-2

640 Piskun, A.S., van de Bovenkamp, H.H., Rasrendra, C.B., Winkelman, J.G.M., Heeres, H.J., 2016.  
641 Kinetic modeling of levulinic acid hydrogenation to  $\gamma$ -valerolactone in water using a carbon  
642 supported Ru catalyst. *Appl. Catal. A-Gen.* 525, 158–167.  
643 <https://doi.org/10.1016/j.apcata.2016.06.033>

644 Pokorný, V., Štejfá, V., Fulem, M., Červinka, C., Růžička, K., 2017. Vapor pressures and  
645 thermophysical properties of ethylene carbonate, propylene carbonate,  $\gamma$ -valerolactone, and  $\gamma$ -  
646 butyrolactone. *J. Chem. Eng. Data* 62, 4174–4186. <https://doi.org/10.1021/acs.jced.7b00578>

647 Protsenko, I.I., Nikoshvili, L.Zh., Matveeva, V.G., Sulman, E.M., 2020. Kinetic modelling of  
648 levulinic acid hydrogenation over ru-containing polymeric catalyst. *Top. Catal.* 63, 243–253.

649 <https://doi.org/10.1007/s11244-020-01223-0>

650 Pulidindi, I.N., Kim, T.H., 2018. Conversion of levulinic acid from various herbaceous biomass  
651 species using hydrochloric acid and effects of particle size and delignification. *Energies* 11, 621.  
652 <https://doi.org/10.3390/en11030621>

653 Qi, L., Horváth, I.T., 2012. Catalytic conversion of fructose to  $\gamma$ -valerolactone in  $\gamma$ -valerolactone.  
654 *ACS Catal.* 2, 2247–2249. <https://doi.org/10.1021/cs300428f>

655 Rodenas, Y., Mariscal, R., Fierro, J.L.G., Alonso, D.M., Dumesic, J.A., Granados, M.L., 2018.  
656 Improving the production of maleic acid from biomass: TS-1 catalysed aqueous phase oxidation  
657 of furfural in the presence of  $\gamma$ -valerolactone. *Green Chem.* 20, 2845–2856.  
658 <https://doi.org/10.1039/C8GC00857D>

659 Saha, N., Al-Muhannadi, R., Al-Mohannadi, A., Véchet, L.N., Castier, M., 2018. Is it the time to  
660 say bye to the  $\phi$ -factor? *Process Saf. Environ.* 113, 193–203.  
661 <https://doi.org/10.1016/j.psep.2017.10.009>

662 Sempere, J., Nomen, R., Serra, R., Cardillo, P., 1997. Thermal hazard assessment using closed-  
663 cell adiabatic calorimetry. *J. Loss Prevent. Proc.* 10, 55–62. <https://doi.org/10.1016/S0950->  
664 [4230\(96\)00035-6](https://doi.org/10.1016/S0950-4230(96)00035-6)

665 Sener, C., Motagamwala, A.H., Alonso, D.M., Dumesic, J.A., 2018. Enhanced furfural yields  
666 from xylose dehydration in the  $\gamma$ -valerolactone/water solvent system at elevated temperatures.  
667 *ChemSusChem* 11, 2321–2331. <https://doi.org/10.1002/cssc.201800730>

668 Serrano-Ruiz, J.C., Wang, D., Dumesic, J.A., 2010. Catalytic upgrading of levulinic acid to 5-  
669 nonanone. *Green Chem.* 12, 574–577. <https://doi.org/10.1039/B923907C>

670 Shen, Y., Zhu, W., Papadaki, M., Mannan, M.S., Mashuga, C.V., Cheng, Z., 2019. Thermal  
671 decomposition of solid benzoyl peroxide using advanced reactive system screening tool: effect of  
672 concentration, confinement and selected acids and bases. *J. Loss Prevent. Proc.* 60, 28–34.  
673 <https://doi.org/10.1016/j.jlp.2019.04.001>

674 Sikorska, D., Macegoniuk, S., Łaszkiewicz, E., Sikorski, P., 2020. Energy crops in urban parks  
675 as a promising alternative to traditional lawns – Perceptions and a cost-benefit analysis. *Urban*  
676 *For. Urban Gree.* 49, 126579. <https://doi.org/10.1016/j.ufug.2019.126579>

677 Singh, J., 1993. Reliable scale-up of thermal hazards data using the PHI-TEC II calorimeter.  
678 *Thermochim. Acta* 226, 211–220. [https://doi.org/10.1016/0040-6031\(93\)80222-V](https://doi.org/10.1016/0040-6031(93)80222-V)

679 Soland, M., Steimer, N., Walter, G., 2013. Local acceptance of existing biogas plants in  
680 Switzerland. *Energy Policy* 61, 802–810. <https://doi.org/10.1016/j.enpol.2013.06.111>

681 Stoessel, F., 2008. Thermal safety of chemical processes, in: Wiley-VCH Verlag GmbH & Co,  
682 Weinheim.

683 Sun, Y., Ni, L., Papadaki, M., Zhu, W., Jiang, J., Mashuga, C., Wilhite, B., Mannan, M.S., 2019.  
684 Process hazard evaluation for catalytic oxidation of 2-octanol with hydrogen peroxide using  
685 calorimetry techniques. *Chem. Eng. J.* 378, 122018. <https://doi.org/10.1016/j.cej.2019.122018>

686 Tang, W., Sarvestani, M., Wei, X., Nummy, L.J., Patel, N., Narayanan, B., Byrne, D., Lee, H.,  
687 Yee, N.K., Senanayake, C.H., 2009. Formation of 2-trifluoromethylphenyl grignard reagent via  
688 magnesium–halogen exchange: Process safety evaluation and concentration effect. *Org. Process*  
689 *Res. Dev.* 13, 1426–1430. <https://doi.org/10.1021/op900040y>

690 Tang, X., Chen, H., Hu, L., Hao, W., Sun, Y., Zeng, X., Lin, L., Liu, S., 2014. Conversion of  
691 biomass to  $\gamma$ -valerolactone by catalytic transfer hydrogenation of ethyl levulinate over metal  
692 hydroxides. *Appl. Catal. B: Environ.* 147, 827–834. <https://doi.org/10.1016/j.apcatb.2013.10.021>

693 Tanwongwan, W., Eiad-ua, A., Kraithong, W., Viriya-empikul, N., Suttisintong, K., Klamchuen,  
694 A., Kasamechonchung, P., Khemthong, P., Faungnawakij, K., Kuboon, S., 2019. Simultaneous  
695 activation of copper mixed metal oxide catalysts in alcohols for gamma-valerolactone production  
696 from methyl levulinate. *Appl. Catal. A: Gen.* 579, 91–98.  
697 <https://doi.org/10.1016/j.apcata.2019.04.011>

698 Tseng, J.-M., Lin, J.-Z., Lee, C.-C., Lin, C.-P., 2012. Prediction of TMCH thermal hazard with

699 various calorimetric tests by green thermal analysis technology. *AIChE J.* 58, 3792–3798.  
700 <https://doi.org/10.1002/aic.13745>

701 Tukacs, J.M., Fridrich, B., Dibó, G., Székely, E., Mika, L.T., 2015. Direct asymmetric reduction  
702 of levulinic acid to gamma-valerolactone: synthesis of a chiral platform molecule. *Green Chem.*  
703 17, 5189–5195. <https://doi.org/10.1039/C5GC01099C>

704 Upham, P., Shackley, S., 2007. Local public opinion of a proposed 21.5MW(e) biomass gasifier  
705 in Devon: Questionnaire survey results. *Biomass Bioenerg.* 31, 433–441.  
706 <https://doi.org/10.1016/j.biombioe.2007.01.017>

707 Valdes, O.R., Moreno, V.C., Waldram, S., Véchet, L., Mannan, M.S., 2016. Runaway  
708 decomposition of dicumyl peroxide by open cell adiabatic testing at different initial conditions.  
709 *Process Saf. Environ.* 102, 251–262. <https://doi.org/10.1016/j.psep.2016.03.021>

710 Veedhi, S., Mishra, V., Kulkarni, S., Gorthi, R., 2014. Incident investigation on thermal instability  
711 of an intermediate using adiabatic calorimeter. *J. Therm. Anal. Calorim.* 115, 909–914.  
712 <https://doi.org/10.1007/s10973-013-3327-5>

713 Veedhi, S., Sawant, A., 2013. Designing a safer process for the reaction of TFA with sodium  
714 borohydride in THF by calorimetric technique. *J. Therm. Anal. Calorim.* 111, 1093–1097.  
715 <https://doi.org/10.1007/s10973-012-2514-0>

716 Vernières-Hassimi, L., Dakkoune, A., Abdelouahed, L., Estel, L., Leveneur, S., 2017. Zero-order  
717 versus intrinsic kinetics for the determination of the time to maximum rate under adiabatic  
718 conditions ( $TMR_{ad}$ ): Application to the decomposition of hydrogen peroxide. *Ind. Eng. Chem.*  
719 *Res.* 56, 13040–13049. <https://doi.org/10.1021/acs.iecr.7b01291>

720 Wang, J., Mannan, M.S., Wilhite, B.A., 2020. Integrated thermodynamic and kinetic model of  
721 homogeneous catalytic N-oxidation processes. *AIChE J.* 66, e16875.  
722 <https://doi.org/10.1002/aic.16875>

723 Wang, Y., Cipolletta, M., Vernières-Hassimi, L., Casson-Moreno, V., Leveneur, S., 2019.

724 Application of the concept of Linear Free Energy Relationships to the hydrogenation of levulinic  
725 acid and its corresponding esters. *Chem. Eng. J.* 374, 822–831.  
726 <https://doi.org/10.1016/j.cej.2019.05.218>

727 Wang, Y., Vernières-Hassimi, L., Casson-Moreno, V., Hébert, J.-P., Leveneur, S., 2018. Thermal  
728 risk assessment of levulinic acid hydrogenation to  $\gamma$ -valerolactone. *Org. Process Res. Dev.* 22,  
729 1092–1100. <https://doi.org/10.1021/acs.oprd.8b00122>

730 Wang, Z., Cao, D., Xu, Z., Wang, J., Chen, L., 2020. Thermal safety study on the synthesis of  
731 HMX by nitrourea method. *Process Saf. Environ.* 137, 282–288.  
732 <https://doi.org/10.1016/j.psep.2020.02.013>

733 Wettstein, S.G., Alonso, D.M., Chong, Y., Dumesic, J.A., 2012. Production of levulinic acid and  
734 gamma-valerolactone (GVL) from cellulose using GVL as a solvent in biphasic systems. *Energy*  
735 *Environ. Sci.* 5, 8199–8203. <https://doi.org/10.1039/C2EE22111J>

736 Wojciechowska, J., Jędrzejczyk, M., Grams, J., Keller, N., Ruppert, A.M., 2019. Enhanced  
737 production of  $\gamma$ -valerolactone with an internal source of hydrogen on Ca-modified TiO<sub>2</sub> supported  
738 Ru catalysts. *ChemSusChem* 12, 639–650. <https://doi.org/10.1002/cssc.201801974>

739 Wong, J.T., 2012. Technological, commercial, organizational, and social uncertainties of a novel  
740 process for vanillin production from lignin. <https://core.ac.uk/download/pdf/56377175.pdf>  
741 (accessed 3 July 2020)

742 Wright, W.R.H., Palkovits, R., 2012. Development of heterogeneous catalysts for the conversion  
743 of levulinic acid to  $\gamma$ -valerolactone. *ChemSusChem* 5, 1657–1667.  
744 <https://doi.org/10.1002/cssc.201200111>

745 Wu, S.-H., Wang, Y.-W., Wu, T.-C., Hu, W.-N., Shu, C.-M., 2008. Evaluation of thermal hazards  
746 for dicumyl peroxide by DSC and VSP2. *J. Therm. Anal. Calorim.* 93, 189–194.  
747 <https://doi.org/10.1007/s10973-007-8874-1>

748 Wu, X., Fu, J., Lu, X., 2012. One-pot preparation of methyl levulinate from catalytic alcoholysis

749 of cellulose in near-critical methanol. *Carbohydr. Res.* 358, 37–39.  
750 <https://doi.org/10.1016/j.carres.2012.07.002>

751 Yan, K., Yang, Y., Chai, J., Lu, Y., 2015. Catalytic reactions of gamma-valerolactone: A platform  
752 to fuels and value-added chemicals. *Appl. Catal. B: Environ.* 179, 292–304.  
753 <https://doi.org/10.1016/j.apcatb.2015.04.030>

754 Zhang, Y., Chung, Y.-H., Liu, S.-H., Shu, C.-M., Jiang, J.-C., 2017. Analysis of thermal hazards  
755 of O,O-dimethylphosphoramidothioate by DSC, TG, VSP2, and GC/MS. *Thermochim. Acta* 652,  
756 69–76. <https://doi.org/10.1016/j.tca.2017.03.014>

757 Zheng, J.L., Wärnå, J., Salmi, T., Burel, F., Taouk, B., Leveneur, S., 2016. Kinetic modeling  
758 strategy for an exothermic multiphase reactor system: Application to vegetable oils epoxidation  
759 using Prileschajew method. *AIChE J.* 62, 726–741. <https://doi.org/10.1002/aic.15037>

760 Zoellner, J., Schweizer-Ries, P., Wemheuer, C., 2008. Public acceptance of renewable energies:  
761 Results from case studies in Germany. *Energy Policy, Transition towards Sustainable Energy*  
762 *Systems* 36, 4136–4141. <https://doi.org/10.1016/j.enpol.2008.06.026>

763